Published in final edited form as:
MRS Bull. 2010 May ; 35(5): 382–388.

Shape and Biomechanical Characteristics of Human Red Blood Cells in Health and Disease

Monica Diez-Silva, **Ming Dao**, **Jongyoon Han**, **Chwee-Teck Lim**, and **Subra Suresh**

Abstract

The biconcave shape and corresponding deformability of the human red blood cell (RBC) is an essential feature of its biological function. This feature of RBCs can be critically affected by genetic or acquired pathological conditions. In this review, we highlight new dynamic *in vitro* assays that explore various hereditary blood disorders and parasitic infectious diseases that cause disruption of RBC morphology and mechanics. In particular, recent advances in high-throughput microfluidic devices make it possible to sort/identify healthy and pathological human RBCs with different mechanobiological characteristics.

Introduction

Advanced new tools have been developed in the past two decades to quantify the mechanical properties of live biological cells. For example, atomic force microscope (AFM), optical (laser) tweezers, and microfluidic devices have been increasingly used to quantify and characterize different mechanobiological signatures at different pathological states for human red blood cells (RBCs). All healthy mammalian RBCs are disc-shaped (discocyte) when not subjected to external stress. The biconcave discocyte RBC has a flexible membrane with a high surface-to-volume ratio that facilitates large reversible elastic deformation of the RBC as it repeatedly passes through small capillaries during microcirculation. RBC deformability is key for circulation, which is necessary to transport oxygen and carbon dioxide. Pathological conditions affecting RBCs can lead to significant alterations to the discocyte shape. Changes to the RBC surface area or membrane properties can compromise cell deformability and disrupt and, in some instances, even obstruct circulation. The consequences of altered circulation often are observed as clinical symptoms that range from benign to lethal (from obstruction of capillaries and restriction of blood flow to tissues to necrosis and organ damage). Here we review a variety of pathological conditions affecting human RBC deformability, including hereditary blood disorders and parasitic infectious diseases, where clinical symptoms related to altered RBC deformability are connected to cell shape morphology changes. For each case, we seek to relate, wherever possible, genetic and molecular level changes caused by a pathologic state to modification of the healthy RBC discocyte shape. We then present *in situ* mechanical testing tools used to quantify the effect on RBC deformability due to different pathological conditions, by recourse to the most recent advances in nanotechnology. We highlight some newly developed microfluidic devices that enable *in situ* high-throughput sorting/identification of human RBCs with different biomechanical properties. We begin with a brief overview of the healthy RBC structure that produces the characteristic discocyte shape.

Healthy Red Blood Cell Structure

The discocyte shape of human RBCs is approximately 7.5 to 8.7 μm in diameter and 1.7 to 2.2 μm in thickness (Figure 1). Hemoglobin molecules, essential for gas transport within the circulation, are contained in the RBC cytosol. The volume of cytosol that is the intracellular

RBC fluid is regulated by the membrane and averages 94 μm^3 at 300 mOsmol/kg (the standard unit osmol measures osmotic pressure as osmols per kilogram [Osmol/kg]; milliosmol [mOsmol] is one-thousandth of one Osmol).[1] The membrane of the RBC comprises a phospholipid bilayer and an underlying two-dimensional network of spectrin molecules. The composite properties of the phospholipid bilayer and spectrin network result in the discocyte morphology of healthy RBCs and give the membrane its elastic and biorheological properties. The bilayer has little shear resistance but contributes to bending resistance and helps to maintain cell surface area. The spectrin network or cytoskeleton is largely responsible for the shear elastic properties of the RBC. Integral and peripheral proteins connect the bilayer and spectrin network. Such connections involving protein binding are referred to as vertical interactions; binding that is involved in the two-dimensional spectrin network formation are referred to as horizontal interactions (Figure 1).[2] Disruptions to vertical and horizontal interactions are known to result in changes to the spectrin network density, which invariably causes cell morphological changes, membrane fluctuations, and RBC deformability for many RBC hereditary disorders.

If one takes the experimentally measured RBC shear modulus and bending modulus, it is, in fact, nontrivial to achieve biconcave shape as the minimum energy configuration.[3,4] Neglecting the significant contribution of strain energy, the biconcave shape can be achieved by bending energy minimization.[5,6] Assuming various zero-energy configurations of the membrane (spontaneous curvature), a stomatocyte (concave RBCs), echinocyte (spiculated RBCs), or discocyte shape was obtained as a possible stable configuration;[4] however, the discocyte shape can only be obtained by fine-tuning the stress-free reference state. Releasing strain energy via dynamic remodeling of the two-dimensional spectrin network of the RBC was shown to enable the biconcave ground state,[3] providing a consistent explanation for accepted elastic moduli values to stabilize the stress-free equilibrium discocyte shape. Li et al.'s full cell spectrin–network RBC model[3] was extended from earlier models of Discher and co-workers.[7,8] The ability to model individual spectrin response and to allow dynamic remodeling in the RBC membrane brought new insights of RBC deformability.

The RBC demonstrates a unique ability for repeated large deformation, which allows for its movement through blood vessels as small as 2–3 μm in diameter during circulation. Dynamic cytoskeleton remodeling of the spectrin network was shown to facilitate this fluidity.[9] These recent studies point to three important factors that influence the structure and mechanical integrity of the spectrin network and the overall shape of the RBC: (1) the shear stress on the RBC membrane, (2) the nature of binding between the vertical interactions and the loss of vertical interactions due to hereditary blood disorders such as spherocytosis (see the Genetic Factors section), and (3) remodeling facilitated by metabolic activity arising from chemical energy. Figure 2 shows the typical results demonstrating chemical energy–assisted cytoskeleton remodeling behavior at two different energy hit rates. Certain sites of the RBC cytoskeleton (e.g., spectrin network) may absorb chemical energy due to contact with energy supplying molecules such as adenosine-5′-triphosphate (ATP). Each energy-supplying molecule carries a certain amount of energy. Therefore, the number of such molecular energy transfer events occurring per unit time can be called the energy hit rate. The spectrin network can have fluidized behavior at higher energy hit rates. The membrane shear strain also influences the “fluidization” (Figure 2a) or “plastic”(Figure 2b) behavior of the spectrin network.[9]

Changes in ATP levels in *in vitro* experimental conditions induce RBC shape changes[4,10] and increase RBC membrane fluctuations.[11] (*In vivo*, ATP changes might result from trauma, infections, RBC hereditary abnormalities, age-related diseases, or cancer.) This dependence was explained in a recent paper,[12] where diffraction phase microscopy showed a direct effect of ATP depletion or addition on the magnitude of RBC membrane

fluctuations. Figure 3 gives the amplitude of membrane fluctuations as influenced by metabolic activity controlled by changes in ATP concentrations. Because RBC fluctuations are directly linked to the membrane bilayer and cytoskeleton network, results suggest that critical binding between the lipid bilayer and spectrin network is actively controlled by ATP.[12] This interaction is attributed to ATP, providing necessary energy for such a dynamic process. Controlling the interaction between the lipid bilayer and spectrin network, ATP is significant in maintaining the characteristic biconcave disc shape of RBCs. Park et al.[12] also observed that in the absence of ATP, a RBC morphological transformation occurs, going from the normal discocyte shape to an echinocyte shape. This morphological transformation is reversible upon restoration of normal levels of ATP. For the remainder of this review, we will focus on cases of pathological conditions that impair RBC deformability through shape and membrane mechanical property modifications.

Genetic Factors

Hereditary Spherocytosis

Hereditary spherocytosis (HS) is a congenital RBC membrane disorder characterized by spherical RBCs that have reduced diameter (microspherocytosis) and are intensely hemoglobinized (carrying more hemoglobin than normal).[13,14] HS is the most common hereditary RBC membrane disorder found. Most affected are Caucasian and Japanese populations.[14] HS is caused by heterogeneous defects in proteins that vertically connect the membrane skeleton to the lipid bilayer. Interactions dependent on vertical connection are thought to play a role in the mechanical stability of the RBC membrane. Mutations responsible for HS include spectrin α and β (SPTA 1 gene and SPTB gene), ankyrin (ANK 1 gene), band 3 (SLC4A 1 gene), protein 4.2 (EPB42 gene), and β–adducing.[15] In HS, abnormalities in the connectivity proteins are accompanied by a decreased spectrin density in the skeleton,[16] which adds to the severity of HS. In healthy RBCs, spectrin molecules bind to actin “nodes” to form a two-dimensional network that constitutes the cytoskeleton. Roughly 5 to 5.5 spectrin molecules bind to each actin filament. However, for HS, loss of spectrin density leads to a reduction in spectrin network connectivity. Network connectivity loss varies based on the specific HS defect that causes loss of membrane mechanical stability, a measurement of the maximum stretch that a membrane can undergo beyond which it is unable to recover its original shape. Spectrin network connectivity can be as low as 3.3 spectrin per actin for cases of HS.[17]

The severity of HS is related to the amount of spectrin network connectivity loss. The increased membrane instability of the HS RBC membrane, due to vertical defects in one of several membrane proteins and isolated spectrin deficiency, promotes the formation of vesicles from the lipid bilayer that is accompanied by membrane loss. Progressive release of vesicles with higher content in lipids than proteins reduces membrane surface area. The process of RBC surface area loss happens more rapidly than volume loss, which results in the formation of spherical RBCs with decreased deformability.[13,14] Lipid loss is thought to take place in the spleen during processing[13] or occur in the bone marrow.[18] Figure 4 shows the deformability index (DI, a quantitative measure of cell ellipticity) of the healthy and spherocyte RBCs as a function of spectrin concentration. DI is determined by ektacytometer measurements (based on laser diffraction analysis where shear stresses can be applied to RBCs in a highly viscous medium). In general, the lower the spectrin density, the smaller the values of DI, the smaller the surface-to-volume ratio, and the smaller the surface area.[19]

Hereditary Elliptocytosis

Hereditary elliptocytosis (HE) describes an inherited group of RBC membrane disorders that result in elliptical, oval, or elongated RBCs. Incidence is difficult to establish because a

majority of HE disorders range from mild clinical symptoms to life-threatening anemia. It is estimated that HE affects about 0.03%–0.05% of the U.S. population.[19] Increases in HE incidence have been observed in Africa, due, in part, to the protection of HE-affected individuals from the malaria disease; however, the precise mechanism by which this occurs is unknown. Although many defects are known to result in HE, cases generally involve disruptions of horizontal cytoskeleton interactions. These defects disrupt the self-association of spectrin tetramers into the cytoskeleton network structure, which leads to reduced elasticity and overall durability of HE RBCs. HE mutations involve Spectrin α and β (SPTA1 gene and SPTB gene) and Protein 4.1 (EPB41 gene). The α-spectrin mutation results in disrupted α-β heterodimer formation. β-spectrin mutations lead to α-β heterodimer incapable of forming spectrin tetramers. Protein 4.1 mutations disrupt spectrin tetramers from binding actin, which results in an improperly formed cytoskeleton scaffold. Horizontal interactions of proteins that form complexes at spectrin junctions are thought to play a role in supporting the structural integrity of the RBC membrane during and after experiencing shear stress. The mutations mentioned previously each lead to horizontal membrane defects causing decreased membrane mechanical stability and reduced deformability of HE RBCs, which can be sufficient to cause hemolytic anemia and RBC fragmentation. Under shear stress, cytoskeleton instability results in destabilization of the entire cytoskeleton network and the formation of elliptocytic/ovalocytic cell shapes. In severe cases, HE RBCs have diminished mechanical integrity compared to healthy RBCs resulting in RBC membrane fragmentation and decreased surface area. HE RBCs are detected and removed from circulation when processed by the spleen. Whereas healthy RBCs circulate for 120 days before clearance by the spleen, HE RBCs have a shorter lifespan due to their intrinsic lower membrane deformability and membrane mechanical instability.

Sickle Cell Disease

Sickle cell disease (SCD) is a group of inherited blood disorders that affect hemoglobin, the protein that carries oxygen in the RBC, and cause sickle-shaped RBCs under specific conditions. Hemoglobin consists of four protein subunits: two α hemoglobin and two β hemoglobin subunits. In the case of SCD, hemoglobin is mutated by substitution of a single amino acid (glutamate by valine) in the β-chain.[20,21] This single change creates an abnormal form of normal hemoglobin (HbA) called sickle cell hemoglobin (HbS). Under low oxygen conditions, HbS binds to itself and aggregates to form long insoluble polymers. Polymerized HbS within deoxygenated sickle RBCs causes a severe morphological change that produces a sickle RBC shape. Sickle cells usually return from the venous circulation to the arterial, where RBCs unsickle as reoxygenation causes HbS to depolymerize. Cycling between sickled and unsickled states causes cells to become dehydrated and dense. After many sickling and unsickling cycles, RBCs lose their ability to recover a discocyte shape upon reoxygenation and become permanently sickled.

Sickle cells display decreased deformability compared to that of normal RBCs[22] and increased intracellular viscosity,[23] affecting the passage of sickled RBCs through small blood vessels, which leads to a decrease in blood flow velocity. HbS polymerization is a key factor of microvascular occlusion, although other rheological factors can also be involved in impaired blood flow. For instance, sickle RBCs exhibit adherence to endothelial cells in the vasculature.[24] In the event sickle RBCs obstruct flow in the microvasculature, reduced blood delivery can lead to organ damage.

A recent advance in understanding sickle cell morphological and rheological changes was completed using *in vitro* microfluidic experiments.[25] By controlling flow pressure and oxygen concentration inside channels the size of capillaries, the investigators reproduced the process of sickling and unsickling SCD cells in well-defined states. In this experiment, SCD cells under normal oxygenated states easily flowed through microchannels. By lowering the

oxygen concentration, sickling of RBCs was observed along with aggregation and blockage within microchannels. Returning to a normal level of oxygenation restored the original shape of RBCs, and normal flow conditions resumed. This experiment is the first *in vitro* reproduction of SCD vascular occlusion and offers great potential to learn more about the connection between SCD sickling shape changes and rheology. The emerging area of microfluidics, like in this sickle cell example, holds great potential for novel *in situ* experiments that can impact medicine. Furthermore, this microfluidic model can be used for clinical applications, such as characterization of drug efficacy to prevent vascular occlusion.

Several forms of SCD exist: inheriting one sickle cell gene from each parent (homozygous, SS); inheriting one sickle cell gene and one gene for another abnormal type of hemoglobin called C (heterozygous, SC); and inheriting one sickle cell gene and one gene for beta thalassemia (heterozygous S-beta thalassemia). The risk of SCD heterozygous populations to suffer severe malaria is 90% less than those who carry no SCD mutations.[26] Thus, despite the high mortality rate associated with SCD, its persistence in populations with ancestry in malaria-risk areas may be explained, in part, by the resistance conferred against this parasitic disease. The precise mechanism by which SCD confers resistance to malaria is unknown.

Parasitic Disease—Malaria

Malaria affects 500 million people and causes more than 1 million deaths per year.[27] While *Plasmodium falciparum* is the species responsible for a majority of malaria-related deaths, *Plasmodium vivax* is globally widespread and remains a morbidity problem. Key to the pathophysiology of falciparum malaria is parasite modification of host RBCs that affects membrane mechanical properties during asexual parasite stages. *P. falciparum*-infected RBCs (*Pf*-RBCs) gradually lose their characteristic biconcave shape, display decreased deformability, and exhibit new cytoadherence properties. Decreased RBC deformability is the combined result of the RBC geometry alteration, parasite proteins insertion into the RBCs membrane, and membrane modifications induced by the parasite.

Modifications of *Pf*-RBCs deformability properties occur minutes after parasite invasion. Few proteins have been identified as contributing to this decrease in deformability. One such parasite protein is RESA (ring-infected erythrocyte surface antigen), which interacts with spectrin following parasite invasion. An optical tweezers study measuring deformability of parasites with a disrupted *resa*1 gene indicated the role of RESA influencing deformability of ring stages.[28] The decrease in deformability contributed by RESA at an early stage of parasite develop ment was more severe at febrile temperatures.[28] Other parasite proteins binding to the RBC cytoskeleton, KAHRP (knob-associated histidine-rich protein) and PfEMP3 (*P. falciparum* Erythrocyte Membrane Protein 3), and *Pf*332[29,30] have been identified through genetic deletion as playing a role in decreased deformability of *Pf*-RBCs observed at late parasite development stages.

The mechanical property changes caused by *P. falciparum* invasion to the RBC have been studied through multiple techniques using ektacytometry,[31,32] and micropipette aspiration.[29,33] New tools have been refined and implemented for the study of *Pf*-RBCs deformation, such as optical tweezers (Figure 5) and diffraction phase microscopy.[28,34–36] The details of these experimental techniques, in addition to other tools frequently used in biological research, are described in recent reviews.[37,38]

In symptomatic human malaria, periodic bouts of intense fever as high as 41°C are a common clinical feature. Optical tweezers and diffraction phase microscopy have been employed to measure the shear modulus of *Pf*-RBCs at physiologic (37°C) and febrile (41°C) temperatures (Figure 6).[28,34–36] In experiments at physiologic conditions, membrane deformability decreased at all *P. falciparum* intra-erythrocytic developmental stages (ring,

trophozoite and schizont). Furthermore, the decrease in membrane deformability was more severe for tests. conducted at febrile temperature (41°C), mimicking a malaria fever *in vitro*.

RBCs infected by mature *P. falciparum* stages cannot be found in the circulation, as they sequester in post-capillary blood vessels of different organs. The reduced deformability of *Pf*-RBCs has a direct effect on impaired flow velocity and consequent flow obstruction. In contrast to *P. falciparum*, remodeling of host RBC membrane structure and consequent mechanical property changes caused by *P. vivax* invasion remains relatively unexplored. *P. vivax* preferentially invades reticulocytes, which are immature RBCs slightly larger than the mature form. Unlike *P. falciparum*, *P. vivax*-infected RBCs (*Pv*-RBCs) do not have cytoadherence properties and slightly sequester. Thus, altered membrane deformability of *Pv*-RBCs could be an important factor for these cells to circulate and avoid splenic clearance. Advances in microfluidic systems have led to *Pf*-RBCs flow studies performed in microfluidic channels that simulate the blood flow and the adhesion encountered by infected RBCs in microcapillaries.[39–41] A recent study using microfluidic technology shows the differences in terms of deformability between uninfected and *Pf*-RBCs and *Pv*-RBCs through constricted channels in flow conditions (Figure 7).[42]

Altered deformability or cytoadherence of *Pf*-RBCs and *Pv*-RBCs influences their circulation and, therefore, plays a role in the balance between parasite sequestration and spleen clearance, ultimately affecting the clinical outcome of the disease. Although mechanisms underlying this process are not completely understood, a pioneering work of *ex vivo* perfusion of human spleen[43] holds potential to give new insights into spleen clearance mechanisms.

Dynamic *In Vitro* Assays

During *P. falciparum* infection, the more mature stages (trophozoite and schizont) are known to cytoadhere and sequester to endothelial cells and accumulate in the microvasculature. Both static and flow adhesion assays have been widely used to investigate sequestration of *Pf*-RBCs. The static adhesion assays usually measure the number of *Pf*-RBCs that remained adhered to a substrate functionalized with host receptors or cells after removal of the nonadherent *Pf*-RBCs so as to identify the specific host receptors and cells and associated parasite proteins that have been involved in cytoadherence.[44–50] On the other hand, flow adhesion assays enable the study of shear stress–mediated adhesion arising from shear flow, which mimics pathophysiologically relevant conditions encountered by the *Pf*-RBCs in circulation.[51–54] However, these traditional flow adhesion assays have their limitations. For example, they are not able to mimic the dimensions of microcapillaries at which sequestration occurs. Microfluidic flow-based assays can better elucidate important details arising from interactions between *Pf*-RBCs with host cells and receptors in enclosed spaces that were previously not possible.[55] Another advantage of using microfluidics technology is that it can easily mimic the variation in shapes of capillaries and network of microvasculature, which will affect the shear flow and, in turn, determine how and where cytoadhesion may occur. For example, microfluidics can model branching capillaries, which are common features in microcirculation. These bifurcations are where changes in flow and shear stress occur; they can reveal the resultant interactions of *Pf*-RBCs with the host receptors and cells that may occur *in vivo* (Figure 8).[40]

Deformability of RBCs (and any other blood cells) is also a key functional characteristic, and human RBC's passage through microcapillaries and spleen sinusoids is a complicated, dynamics process involving such repeated deformations. Many *in vivo* factors affecting this process are not clearly known or studied, and *in vivo* visualization of healthy and diseased RBC movement through microcapillaries or the spleen is impossible at this time.

Microfluidics technology can provide an ideal experimental platform for studying cell biorheological properties and also serve as an ideal *in vitro* model for these physiological biofiltration processes, as this technology can approximate the smallest dimensions that human RBCs pass through.

The idea of using microstructures as artificial filters dates back to the mid-1990s,[56] enabled by the demonstrated ability to fabricate a micrometer-sized structure at a reasonable cost. Adopting the same idea for the problem of malaria-infected RBCs, in a manner that mimics the *in vivo* physiological processes,[39–42] is good demonstration of the potential of the technology. Not only can one obtain important biophysical insights from these experiments, they have the potential to be useful as a screening tool for potential new therapeutic interventions. The importance of such *in vitro* model systems in studying biorheology of human blood cells will only increase in coming years.

Another use of microfluidic systems will be mechanical cell sorting, as an alternative to well-established fluorescence-activated cell sorting (FACS) or magnetic sorting. While FACS and related cell sorting techniques are based on the chemical affinity (of cell surface markers), microfluidic structures can be used to sort cells based on physical/mechanical properties, such as size, shape, and deformability. This can perhaps be motivated by the fact that affinity-based cell sorting is often inadequate for dealing with certain problems, such as varying or heterogeneous expression of cell surface markers. Thus, motivation for these mechanical cell–sorting devices is that they do not require chemical labels (antibodies to cell surface markers) or complicated sample preparation processes.

Various physical cell-sorting microfluidic devices have been demonstrated, utilizing physical interaction with microscopic pillars[57] and channel walls,[58] inertial forces on blood cells,[59] and biomimetic cell margination (Fahraeus-Lindqvist effect, Figure 9).[60] Many of these devices are “inspired” by the *in vivo* physiological cell interactions in spleen and blood vessels, which, in return, renders the result of the separation/sorting by these techniques more physiologically relevant. For example, both ring-stage *Pf*-RBCs were separated (based on mechanical deformability) from normal RBCs in a continuous-flow fashion by carefully designing 2.2-μm microfilters in an anisotropic filter array design.[61] Such a tool would find significant use in studying the pathophysiology and disease process of malaria parasite in different stages.

Conclusion and Outlook

Various biomechanical properties of human RBCs are important functional biomarkers, with significant potential for application in biological/clinical research. With the advent of microfluidics technology, research into the biomechanical response of human blood cells in health and disease has benefited significantly from both ideal *in vitro* model systems that mimic complex *in vivo* physiological cell deformation processes and microfluidic toolkits for mechanical cell sorting and profiling that would facilitate sample preparation and detection. However, in order to make a much broader impact, two major technical issues need to be resolved. First, the current throughput of microfluidic cell mechanical measurement is still relatively low, limiting the possibility of obtaining data with good statistics. Second, such a measurement should be carried out on an individual cell (but over a large population of cells) without suffering from cell-to-cell interaction and clogging.

Microfluidic biomechanical sorting of RBCs provides an interesting alternative for more conventional affinity-based sorting, since it does not require any affinity reagents (antibodies) and is not sensitive to any chemical/thermal degradation. This is especially meaningful for the disease diagnostics in remote, resource-limited settings where typical lab

infrastructure is not available. Coupled with the biological/biomechanical study of RBCs, this application area is expected to receive much more attention in the coming years.

Acknowledgments

We acknowledge support from the Interdisciplinary Research Groups on Infectious Diseases (ID) and BioSystems and Micromechanics (BioSyM), which is funded by the Singapore-MIT Alliance for Research and Technology (SMART), support from the Advanced Materials for Micro and Nano Systems Programme and the Computational Systems Biology Programme of the Singapore-MIT Alliance, and support from Global Enterprise for Micro-Mechanics and Molecular Medicine (GEM4) Laboratory at the National University of Singapore. S.S. acknowledges support from the National Institute of Health (Grants R01 HL094270-01A1 and 1-R01-GM076689-01) and support from the National University of Singapore through Tan Chin Tuan Centennial Overseas Chair professorship.

References

1. Fung, YC. Biomechanics: Mechanical Properties of Living Tissues. Springer-Verlag; New York: 1993.
2. Tse WT, Lux SE. Br J Haematol 1999;104:2. [PubMed: 10027705]
3. Li J, Dao M, Lim CT, Suresh S. Biophys J 2005;88:3707. [PubMed: 15749778]
4. Lim HWG, Wortis M, Mukhopadhyay R. Proc Nat Acad Sci U S A 2002;99:16766.
5. Canham PB. J Theor Biol 1970;26:61. [PubMed: 5411112]
6. Helfrich W. Z Naturforsch, C: Biosci 1973;C 28:693.
7. Discher DE, Boal DH, Boey SK. Phys Rev E 1997;55:4762.
8. Discher DE, Boal DH, Boey SK. Biophys J 1998;75:1584. [PubMed: 9726959]
9. Li J, Lykotrafitis G, Dao M, Suresh S. Proc Nat Acad Sci U S A 2007;104:4937.
10. Wong P. J Theor Biol 1999;196:343. [PubMed: 10049626]
11. Gov NS, Safran SA. Biophys J 2005;88:1859. [PubMed: 15613626]
12. Park YK, Best CA, Auth T, Gov N, Safran G, Popescu G, Suresh S, Feld MS. Proc Nat Acad Sci U S A 2010;107:1289.
13. Eber S, Lux SE. Semin Hematol 2004;41:118. [PubMed: 15071790]
14. Perrotta S, Gallagher PG, Mohandas N. Lancet 2008;372:1411. [PubMed: 18940465]
15. Gallagher PG. Curr Hematol Rep 2004;3:85. [PubMed: 14965483]
16. Becker PS, Lux SE. Clin Haematol 1985;14:15. [PubMed: 3886234]
17. Liu SC, Derick LH, Agre P, Palek J. Blood 1990;76:198. [PubMed: 2364170]
18. Da Costa L, Mohandas N, Sorette M, Grange MJ, Tchernia G, Cynober T. Blood 2001;98:2894. [PubMed: 11698268]
19. Walensky, LD.; Narla, M.; Lux, SE. Blood: Principles and Practice of Hematology. 2nd. Handin, RI.; Lux, SE.; Stossel, TP., editors. Lippincott Williams, and Wilkins; Philadelphia: 2003. p. 1709
20. Pauling L, Itano HA, Singer SJ, Wells IC. Science 1949;110:543. [PubMed: 15395398]
21. Ingram VM. Nature 1956;178:792. [PubMed: 13369537]
22. Embury, SH.; Hebbel, RP.; Steinberg, MH.; Mohandas, N. Sickle Cell Disease. Embury, SH.; Hebbel, RP.; Mohandas, N.; Steinberg, MH., editors. Raven Press; New York: 1994. p. 311
23. Mohandas, N.; Hebbel, RP. Sickle Cell Disease. Embury, SH.; Hebbel, RP.; Mohandas, N.; Steinberg, MH., editors. Raven Press; New York: 1994. p. 205
24. Hebbel RP, Yamada O, Moldow CF, Jacob HS, White JG, Eaton JW. J Clin Invest 1980;65:154. [PubMed: 7350195]
25. Higgins JM, Eddington DT, Bhatia SN, Mahadevan L. Proc Nat Acad Sci U S A 2007;104:20496.
26. Hill AVS, Allsopp CEM, Kwiatkowski D, Anstey NM, Twumasi P, Rowe PA, Bennett S, Brewster D, McMichael AJ, Greenwood BM. Nature 1991;352:595. [PubMed: 1865923]
27. Greenwood A, Mutabingwa B, Malaria T. Nature 2002;415:670. [PubMed: 11832954]
28. Mills JP, Diez-Silva M, Quinn DJ, Dao M, Lang MJ, Tan KSW, Lim CT, Milon G, David PH, Mercereau-Puijalon O, Bonnefoy S, Suresh S. Proc Nat Acad Sci U S A 2007;104:9213.

29. Glenister FK, Coppel RL, Cowman AF, Mohandas N, Cooke BM. Blood 2002;99:1060. [PubMed: 11807013]
30. Glenister FK, Fernandez KM, Kats LM, Hanssen E, Mohandas N, Coppel RL, Cooke BM. Blood 2009;113:919. [PubMed: 18832660]
31. Cranston HA, Boylan CW, Carroll GL, Sutera SP, Williamson JR, Gluzman IY, Krogstad DJ. Science 1984;223:400. [PubMed: 6362007]
32. Dondorp AM, Angus BJ, Hardeman MR, Chotivanich KT, Silamut K, Ruangveerayuth R, Kager PA, White NJ, Vreeken J. Am J Trop Med Hyg 1997;57:507. [PubMed: 9392587]
33. Paulitschke M, Nash GB. J Lab Clin Med 1993;122:581. [PubMed: 8228577]
34. Suresh S, Spatz J, Mills JP, Micoulet A, Dao M, Lim CT, Beil M, Seufferlein T. Acta Biomater 2005;1:15. [PubMed: 16701777]
35. Mills, JP.; Qie, L.; Dao, M.; Tan, KSW.; Lim, CT.; Suresh, S. Mechanical Properties of Bioinspired and Biological Materials. Viney, C.; Katti, K.; Ulm, FJ.; Hellmich, C., editors. Vol. 844. 2005. p. 179
36. Park YK, Diez-Silva M, Popescu G, Lykotrafitis G, Choi WS, Feld MS, Suresh S. Proc Nat Acad Sci U S A 2008;105:13730.
37. Bao G, Suresh S. Nat Mater 2003;2:715. [PubMed: 14593396]
38. Van Vliet KJ, Li J, Zhu T, Yip S, Suresh S. Phys Rev B 2003;67
39. Shelby JP, White J, Ganesan K, Rathod PK, Chiu DT. Proc Nat Acad Sci U S A 2003;100:14618.
40. Antia M, Herricks T, Rathod PK. PLoS Pathog 2007;3:939.
41. Herricks T, Antia M, Rathod PK. Cell Microbiol 2009;11:1340. [PubMed: 19438513]
42. Handayani S, Chiu DT, Tjitra E, Kuo JS, Lampah D, Kenangalem E, Renia L, Snounou G, Price RN, Anstey NM, Russell B. Journal of Infectious Diseases 2009;199:445. [PubMed: 19090777]
43. Safeukui I, Correas JM, Brousse V, Hirt D, Deplaine G, Mule S, Lesurtel M, Goasguen N, Sauvanet A, Couvelard A, Kerneis S, Khun H, Vigan-Womas I, Ottone C, Molina TJ, Treluyer JM, Mercereau-Puijalon O, Milon G, David PH, Buffet PA. Blood 2008;112:2520. [PubMed: 18579796]
44. Udeinya IJ, Schmidt JA, Aikawa M, Miller LH, Green I. Science 1981;213:555. [PubMed: 7017935]
45. Ockenhouse CF, Tandon NN, Magowan C, Jamieson GA, Chulay JD. Science 1989;243:1469. [PubMed: 2467377]
46. Roberts DD, Sherwood JA, Spitalnik SL, Panton LJ, Howard RJ, Dixit VM, Frazier WA, Miller LH, Ginsburg V. Nature 1985;318:64. [PubMed: 2414670]
47. Berendt AR, Simmons DL, Tansey J, Newbold CI, Marsh K. Nature 1989;341:57. [PubMed: 2475784]
48. Oquendo P, Hundt E, Lawler J, Seed B. Cell 1989;58:95. [PubMed: 2473841]
49. Baruch DI, Gormley JA, Ma C, Howard RJ, Pasloske BL. Proc Nat Acad Sci U S A 1996;93:3497.
50. Rowe JA, Moulds JM, Newbold CI, Miller LH. Nature 1997;388:292. [PubMed: 9230440]
51. Cooke BM, Berendt AR, Craig AG, Macgregor J, Newbold CI, Nash GB. Br J Haematol 1994;87:162. [PubMed: 7524615]
52. Yipp BG, Anand S, Schollaardt T, Patel KD, Looareesuwan S, Ho M. Blood 2000;96:2292. [PubMed: 10979979]
53. Gray C, McCormick C, Turner G, Craig A. Mol Biochem Parasitol 2003;128:187. [PubMed: 12742585]
54. Cooke BM, Glenister FK, Mohandas N, Coppel RL. Br J Haematol 2002;117:203. [PubMed: 11918556]
55. Antia M, Herricks T, Rathod PK. Cell Microbiol 2008;10:1968. [PubMed: 18754851]
56. Brody JP, Han Y, Austin RH, Bitensky M. Biophys J 1995;68:2224. [PubMed: 7647230]
57. Davis JA, Inglis DW, Morton KJ, Lawrence DA, Huang LR, Chou SY, Sturm JC, Austin RH. Proc Nat Acad Sci U S A 2006;103:14779.
58. Takagi J, Yamada M, Yasuda M, Seki M. Lab Chip 2005;5:778. [PubMed: 15970972]

59. Di Carlo D, Edd JF, Irimia D, Tompkins RG, Toner M. Anal Chem 2008;80:2204. [PubMed: 18275222]
60. Shevkoplyas SS, Yoshida T, Munn LL, Bitensky MW. Anal Chem 2005;77:933. [PubMed: 15679363]
61. Bow, H.; Hou, HW.; Goldfless, S.; Abgrall, P.; Tan, KSW.; Niles, J.; Lim, CT.; Han, J. Proceedings of the MicroTAS 2009 conference; Jeju, Korea. 2009; p. 1219
62. Suresh S. J Mater Res 2006;21(8):1871.

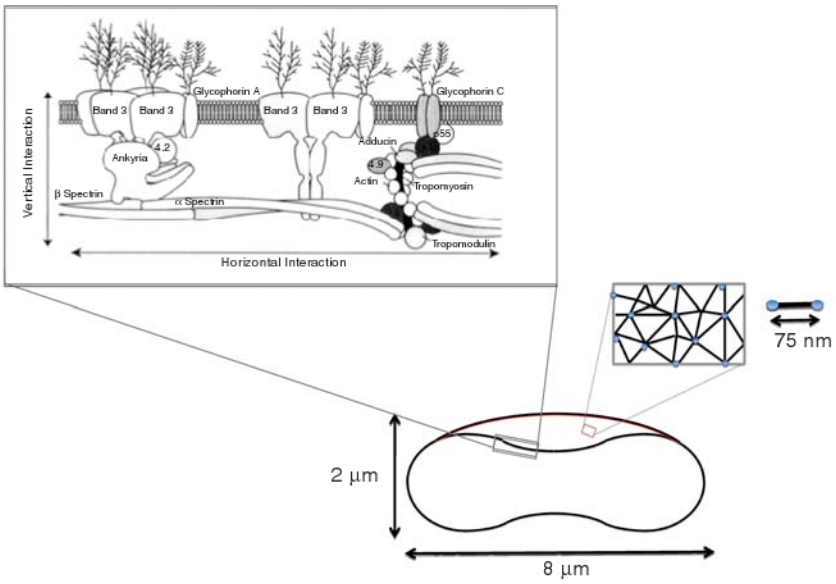

Figure 1.

Schematic representation of a healthy red blood cell (RBC) membrane, geometry (discocyte shape), and spectrin network. Upper left inset shows the cross-sectional view of the RBC membrane with vertical and horizontal interactions. Right inset shows the two-dimensional connectivity of the spectrin network. Reprinted with permission from [Reference 2]. ©1999, Wiley.

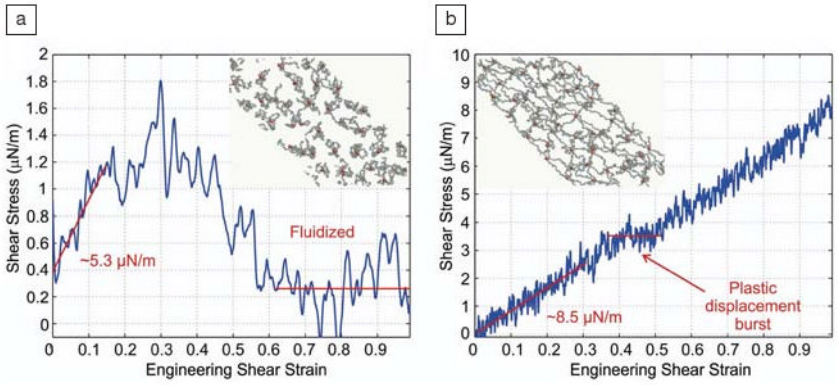

Figure 2.

Shear stress-strain response of a spectrin network at a strain rate of 3×10^5 per s. (a) Energy hit rate 10 per s and final network structure (inset) at 100% shear strain. (b) Energy hit rate 2.5 per s and final network structure (inset) at 100% shear strain. Reprinted with permission from Reference 9. ©2007, National Academy of Sciences.

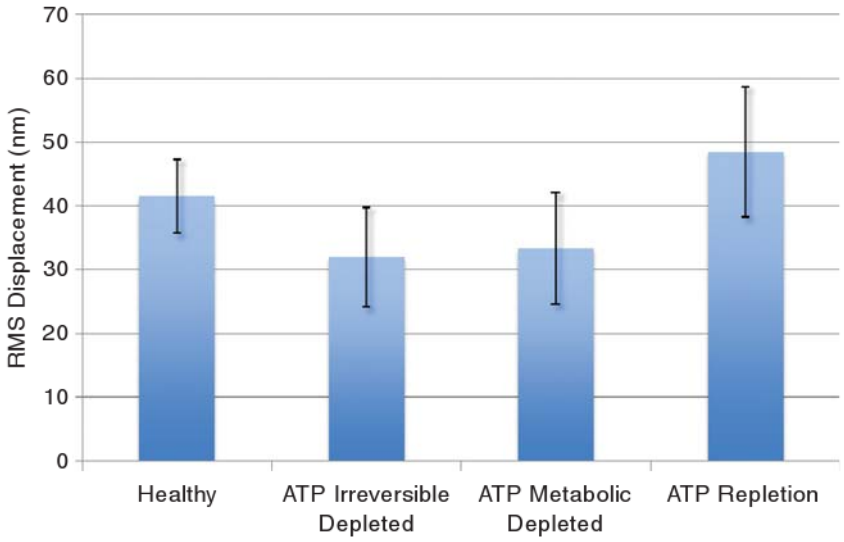

Figure 3.

Effect of adenosine-5′-triphosphate (ATP) on membrane fluctuations measured by root mean squared (RMS) displacement of red blood cell membrane. When ATP is depleted, irreversibly or metabolically, membrane fluctuations decrease, and echinocyte shape is observed. When ATP levels are restored, normal fluctuation behavior and biconcave shape returns. Adapted from [Reference 12].

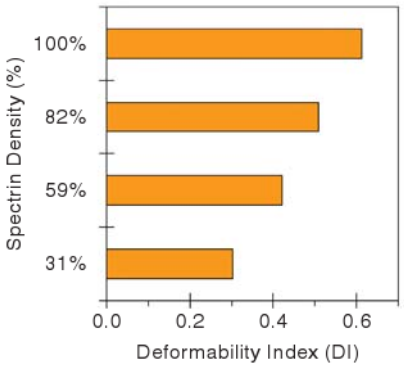

Spectrin Density	Relative Surface-to-Volume Ratio	Relative Surface Area
100% (healthy RBC)	Large	Large
82%	Small	Small
59%	Smaller	Smaller
31%	Smallest	Smallest

Figure 4.

Deformability of the healthy and spherocyte red blood cells (RBCs) as a function of spectrin concentration at a fixed osmolality of 300 mOs mol/kg. The lower the spectrin density, the smaller the deformability index (DI) values, surface-to-volume ratio, and surface area. In more hypotonic solutions (lower osmolality), a decrease in surface-to-volume ratio causes a reduction in DI at a fixed spectrin density. In hypertonic solutions (higher osmolality), cellular dehydration results in lower DI. Adapted from [Reference 19].

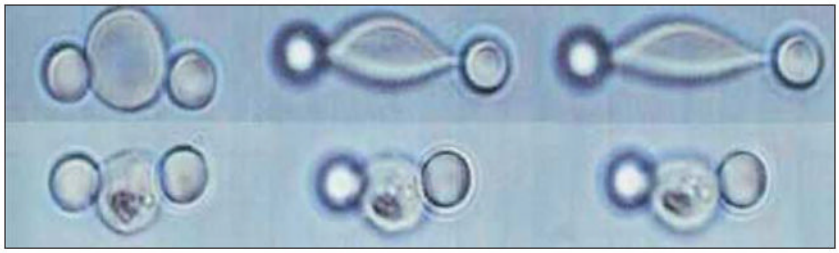

Figure 5.
Controlled stretching using an optical trap of healthy (top) and infected (bottom) red blood cells (RBCs). The left lighted bead indicates that it was trapped by the laser, while the right bead was adhered to the glass cover slip. Bottom row shows how stiff the late-stage *P. falciparum*–infected RBC (*Pf*-RBCs) had become when compared with its healthy counterpart shown in the top row undergoing the same stretching force.[34,62] (Bead diameter is 4 μm.) Reprinted with permission from Reference 34. ©2005, Elsevier.

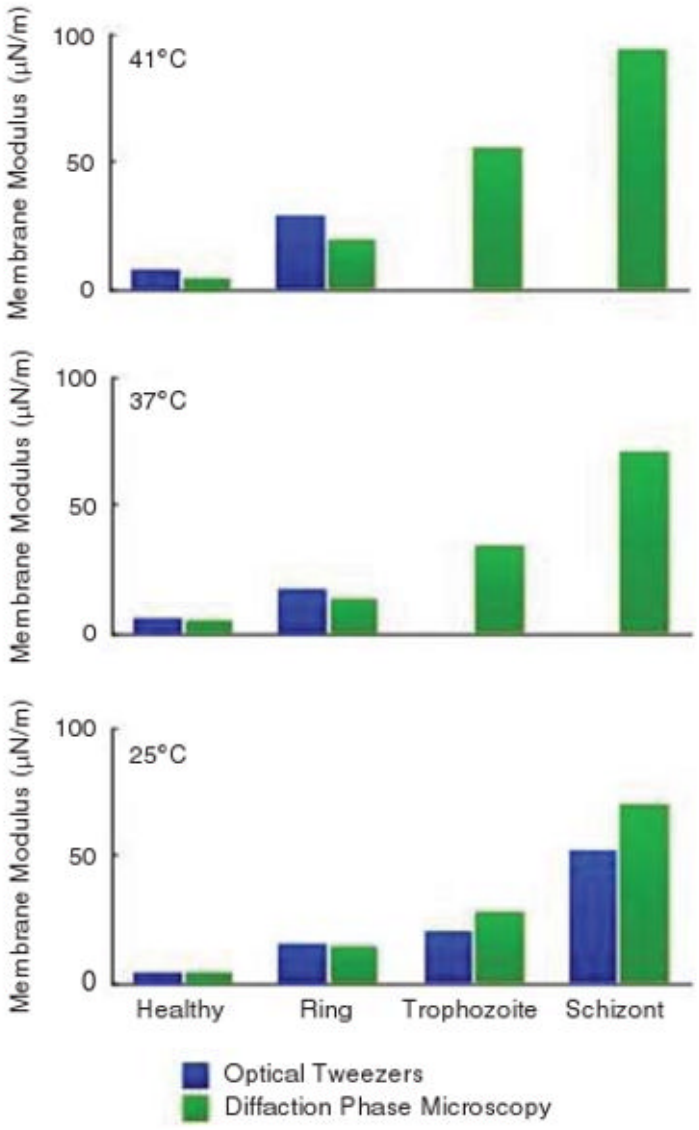

Figure 6.

Shows the shear modulus response of infected red blood cell (RBC) membrane as a function of the *P. falciparum* intra-erythrocytic developmental cycle (ring, trophozoite, and schizont stages) and temperature. Data from two independent experimental techniques, optical tweezers and diffraction phase microscopy, show good agreement.[28,35,36]

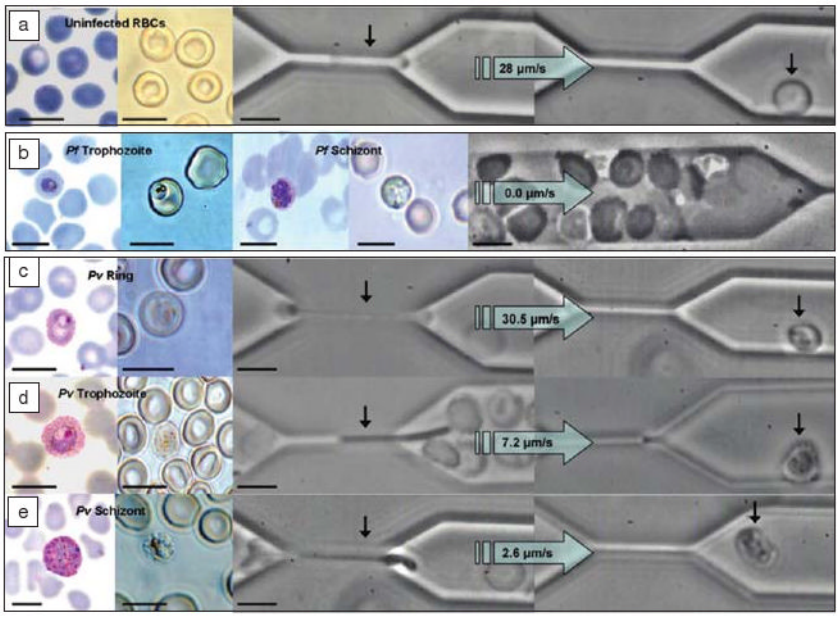

Figure 7.

Passage of (a) uninfected, (b) trophozoite, and schizont stages of *P. falciparum*–infected red blood cells (RBCs) (*Pf*-RBCs) and (c–e) ring, trophozoite, and schizont stages of *P. vivax*–infected RBCs (*Pv*-RBCs) through 2 μm constricted channels. Scale bar = 10 μm in all cases. Reprinted with permission from Reference 42. ©2009, University of Chicago Press.

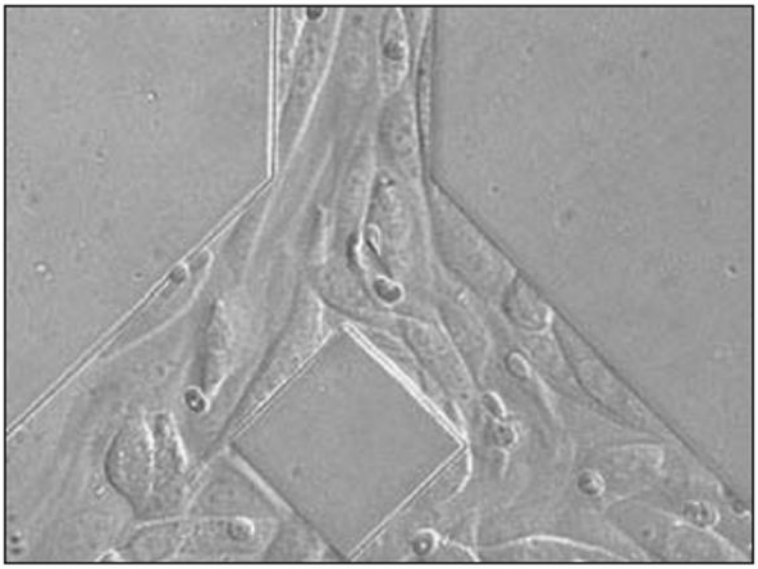

Figure 8.
A bifurcated micochannel showing cyto-adhered *P. falciparum* infected RBC (*Pf*-RBCs). The microchannel has been seeded with Chinese Hamster Ovary (CHO) cells expressing CD-36 human receptor. (*Pf*-RBCs average diameter of 7.5 μm). Reprinted with permission from [Reference 55]. ©2008, Wiley.

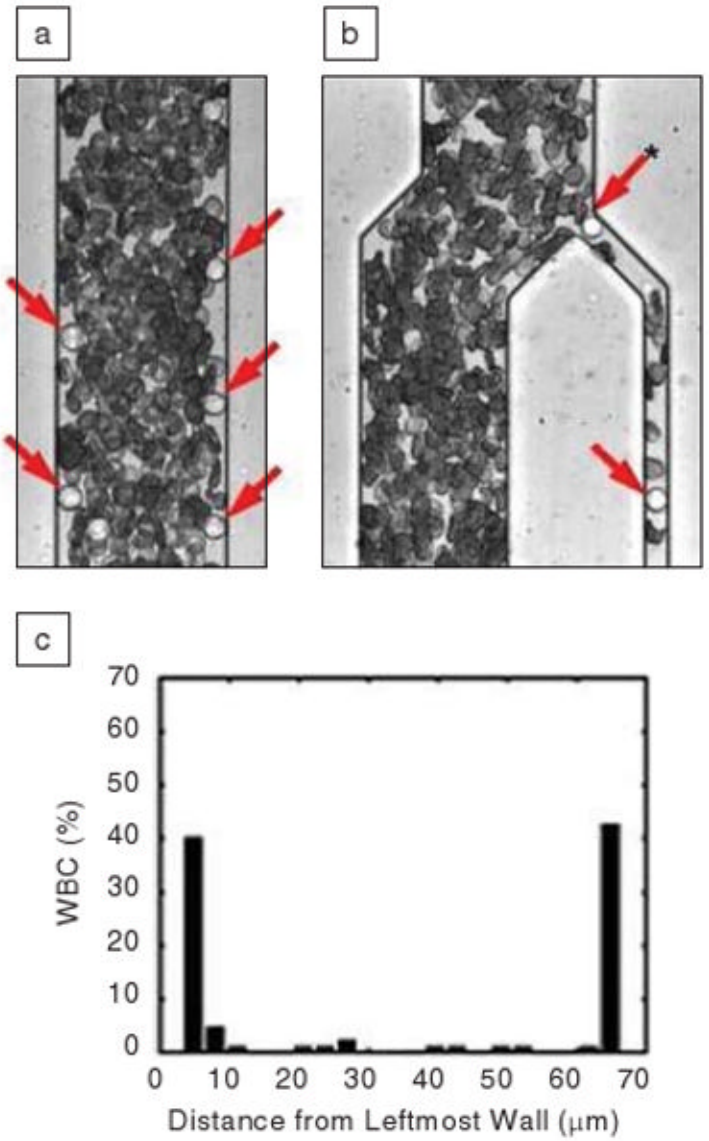

Figure 9.

Microfluidic blood cell sorting using the Fahraeus effect. (a) In a 5.5-mm long rectangular, straight microchannel leukocytes will be marginated to the edge, while more flexible red blood cells (RBCs) are concentrated in the center. (b) Using a bifuricated channel, one can sample and enrich white blood cells (WBCs), which are indicated by arrows. (c) The separation process is determined by both size and deformability of the WBC, compared with RBC. Reprinted with permission from [Reference 60]. ©2005, American Chemical Society.